Materials Research Bulletin 51 (2014) 432–437

Contents lists available at ScienceDirect

Materials Research Bulletin

journal homepage: www.elsevier.com/locate/matresbu

Synthesis of g-C_3N_4/Ag_3PO_4 heterojunction with enhanced photocatalytic performance

Peizhi He [a], Limin Song [a,*], Shujuan Zhang [b,*], Xiaoqing Wu [c,*], Qingwu Wei [a]

[a] College of Environment and Chemical Engineering & State Key Laboratory of Hollow-Fiber Membrane Materials and Membrane Processes, Tianjin Polytechnic University, Tianjin 300387, PR China
[b] College of Science, Tianjin University of Science & Technology (co-first institution), Tianjin 300457, PR China
[c] Institute of Composite Materials & Ministry of Education Key Laboratory of Advanced Textile Composite Materials, Tianjin Polytechnic University, Tianjin 300387, PR China

ARTICLE INFO

Article history:
Received 11 September 2013
Received in revised form 23 December 2013
Accepted 30 December 2013
Available online 8 January 2014

Keywords:
A. Inorganic compound
B. Chemical synthesis
D. Catalytic properties

ABSTRACT

g-C_3N_4/Ag_3PO_4 heterojunction photocatalyst with visible-light response was prepared by a facile coprecipitation method. The photocatalysts were characterized by X-ray powder diffraction, transmission electron microscopy, UV–vis absorption spectroscopy and Fourier transform infrared spectroscopy. The photocatalytic activities of the obtained samples were tested by using Rhodamine B (RhB) as the degradation target under visible light irradiation. g-C_3N_4/Ag_3PO_4 decomposed RhB more effectively than the pure Ag_3PO_4 particles did, and 2 wt.% g-C_3N_4 had the highest activity. Furthermore, 2 wt.% g-C_3N_4/Ag_3PO_4 degraded high-concentration RhB more potently than unmodified Ag_3PO_4 did, probably because g-C_3N_4/Ag_3PO_4 heterojunction photocatalyst enhanced the photocatalytic activity by efficiently separating the photogenerated electron–hole pairs.

1. Introduction

Photocatalytic semiconductors have attracted worldwide attention for renewable energy and clean environment in various systems [1], of which TiO_2 is most frequently used due to efficient photocatalytic activity, inexpensiveness, chemical stability and harmlessness. However, TiO_2 can only absorb UV light accounting for about 3% of the solar spectrum [2]. Therefore, it is necessary to synthesize highly-active and visible-light response photocatalysts. For instance, Zou et al. developed efficient photocatalysts so as to effectively utilize solar energy [3].

Silver orthophosphate (Ag_3PO_4), a highly active visible-light-energized photocatalyst, can utilize visible light to oxidize water and to decompose organic contaminants in aqueous solution [4]. By using density-functional-theory-based calculations, Umezawa et al. reported that PO_4 tetrahedral units promoted the carrier transfer to surface by inhibiting the hybridization of Ag4d and O2p. Theoretically, Ag_3PO_4 is of high photocatalytic activity [5]. In practice, photocatalytic activity can be boosted by preparing silver phosphate with different protocols, including hybridization, morphology control [6–9], size control [10] and modification [11–15].

As a metal-free semiconductor, graphitic carbon nitride (g-C_3N_4) is potentially applicable for the high thermal, chemical stability, as well as versatile optical, electronic and catalytic properties [16–18]. In 2009, Wang et al. first reported that g-C_3N_4 produced hydrogen from water under visible-light irradiation. g-C_3N_4, which is capable of harvesting light sufficiently [19], can be synthesized by heating dicyandiamide, and pressurizing hot and supercritical fluid, etc. [20]. Wang et al. also synthesized hollow nanospheres as light-harvesting antennae and nanostructured scaffolds in the optical range [21]. Moreover, g-C_3N_4 is prone to forming doped or heterojunction compound because of the smallest band gap among various C_3N_4 [22,23].

Herein, we endeavoured to synthesize Ag_3PO_4 nanomaterials by a precipitation method and efficient visible-light-sensitized g-C_3N_4/Ag_3PO_4 composites with different weight percents of g-C_3N_4 by a simple coprecipitation method. Under visible light irradiation, 2 wt.% g-C_3N_4/Ag_3PO_4 composite photocatalyst managed to dramatically enhance the photocatalytic activity against RhB, especially high-concentration RhB, compared with pure Ag_3PO_4 nanospheres did. In this study, g-C_3N_4/Ag_3PO_4 heterojunction photocatalyst functioned potently by separating photogenerated electron–hole pairs efficiently. A similar g-C_3N_4/Ag_3PO_4 composite photocatalyst has been reported [24], and 2 wt.% g-C_3N_4/Ag_3PO_4 was appropriate for the degradation of high-concentration RhB.

* Corresponding authors. Tel.: +86 22 83955458; fax: +86 22 83955458.
E-mail addresses: songlmnk@sohu.com, songlimin@tjpu.edu.cn, tjpu2013@sohu.com (S. Zhang).

0025-5408/$ – see front matter © 2014 Published by Elsevier Ltd.
http://dx.doi.org/10.1016/j.materresbull.2013.12.064

2. Experiment

2.1. Chemicals

All the reagents were obtained from Tianjin Chemical Co., Ltd. All the chemicals were of analytical reagent grade and used without being purified. Deionized water was used throughout the experiments.

2.2. Preparation of g-C_3N_4

g-C_3N_4 powders were synthesized by heating dicyandiamide in a home-made tube furnace at 2000 W. In a typical procedure, 2 g dicyandiamide was placed in two porcelain boats placed in the middle of the tube furnace, heated from 25 °C to 550 °C at the rate of 20 °C/min, and kept at 550 °C for 4 h in a flowing N_2 at the rate of 10 mL/min. After the tube furnace was cooled to room temperature, the product was ground, washed by deionized water several times, and separated by suction filtration. After vacuum-drying at 80 °C for 4 h, g-C_3N_4 was obtained as yellow powders.

2.3. Synthesis of g-C_3N_4/Ag_3PO_4 photocatalyst

g-C_3N_4/Ag_3PO_4 photocatalysts with the g-C_3N_4 contents of 0.5 wt.%, 1 wt.%, 2 wt.%, 3 wt.% and 4 wt.% respectively were prepared by a coprecipitation method. For example, for the 2 wt.% sample, 0.358 g $AgNO_3$ was dissolved in 10 mL of deionized water, i.e. 0.143 g $(NH_4)_3PO_4{\cdot}3H_2O$. The latter was dripped slowly into the former under magnetic stirring. The mixture was stirred vigorously for 0.5 h at room temperature, and then appropriate amount of g-C_3N_4 was added and stirred for 0.5 h. The product was separated from the solution by centrifuge, washed three times with deionized water to remove excess reaction reagents, and then vacuum-dried at 80 °C overnight.

2.4. Characterization of g-C_3N_4/Ag_3PO_4 photocatalyst

Photocatalyst powders were characterized by using X-ray diffraction (XRD) on a Rigaku D/max 2500 powder diffractometer equipped with monochromatic high-intensity Cu Kα radiation (λ = 1.5406 Å). Transmission electron microscopy (TEM) images of the as-prepared products were obtained by a Hitachi H-7650 electron microscope. UV–vis absorption spectra for estimating photophysical properties were recorded on an HP8453 spectrophotometer equipped with an integration sphere, with $BaSO_4$ as the reference. Fourier transform infrared spectroscopy (FTIR) was recorded on a TENSOR37 near-infrared spectrometer (BRUKER) using potassium bromide (KBr) pellet. Photoluminescence spectra (PL) were acquired using a Cary Eclipse photoluminescence analyzer.

2.5. Catalytic activity evaluation

The photocatalytic activities of various samples under visible-light irradiation were estimated by using RhB as the model substrate. In a typical process, 100 mL of RhB (10 mg/L) aqueous solution and 0.1 g photocatalyst powders were mixed in a 250 mL photoreactor. Prior to irradiation, the photocatalyst suspension was immersed in the same solution for 0.5 h in dark to reach adsorption–desorption equilibration. A 300 W Xe lamp (80 mW/cm^2) with a 420 nm cutoff filter was used as the simulated solar light source and the spectrum of the final light after a quartz container was $\lambda > 400$ nm. The above suspension with air blown at the flow rate of 100 mL/min was photoirradiated under continuous stirring. The residual concentrations of RhB after irradiation were evaluated at regular intervals according to the absorbance at 552 nm. The degradation rate of RhB was calculated by $(A_0 - A)/A_0 \times 100\%$.

OH was detected by the terephthalic acid ($C_8H_6O_4$, TA) fluorescence method. OH can react with TA and generate TAOH which emits fluorescence at around 426 nm according to the equation [25]:

$$OH + TA \rightarrow TAOH$$

An 80 mL of 3 mM terephthalic acid and 0.1 M NaOH aqueous solution was prepared, and then 5 mg as-prepared photocatalyst powders were mixed in a 250 mL quartz photoreactor. The photocatalyst suspension was immersed in the same solution for 0.5 h in dark to reach adsorption–desorption equilibration as the foregoing. The photoreaction was carried out under visible light without air bubbled, and the suspension was quantitatively sampled at regular intervals.

3. Results and discussion

3.1. Characterization of 2 wt.% g-C_3N_4/Ag_3PO_4 and pure Ag_3PO_4

In order to analyze the structure and phase composition of the photocatalyst, powder XRD study was carried out. The XRD patterns of pure Ag_3PO_4, g-C_3N_4, 2 wt.% g-C_3N_4/Ag_3PO_4 and 4 wt.% g-C_3N_4/Ag_3PO_4 are shown in Fig. 1. All the peaks can be well indexed to the cubic-phase Ag_3PO_4 (JCPDS Card No. 06-0505 $a = b = c = 6.007$ Å). The diffraction pattern of Ag_3PO_4 shows peaks at 21.1°, 29.9°, 33.5°, 36.8°, 42.7°, 48.0°, 52.9°, 55.2°, 57.5°, 61.8°, 66.0°, 70.1°,72.1° and 74.0°, which correspond to planes (1 1 0), (2 0 0), (2 1 0), (2 1 1), (2 2 0), (3 1 0), (2 2 2), (3 2 0), (3 2 1), (4 0 0), (3 3 0), (4 2 0), (4 2 1) and (3 2 2), respectively. There are no peaks of impurities, and the sharp peaks demonstrate that the samples crystallize well. In the g-C_3N_4 diffraction patterns, the most intense XRD peak at 27.4°, which corresponds to the (0 0 2) peak in accordance with an interlayer distance of 0.326 nm, can be attributed to the stacking of the conjugated aromatic system [19,26]. In the 2 wt.% g-C_3N_4/Ag_3PO_4 and 4 wt.% g-C_3N_4/Ag_3PO_4 diffraction patterns, negligible peaks representing slice-like g-C_3N_4 can be detected, which has been reported before [27].

The morphological and microstructural details of the as-prepared samples were examined by TEM (Fig. 2). Fig. 2(a) presents the TEM image of reunited spherical Ag_3PO_4 with the diameters of approximately 150–400 nm, which matches the XRD data. g-C_3N_4 has a slice-like morphology (Fig. 2(b)), being similar to

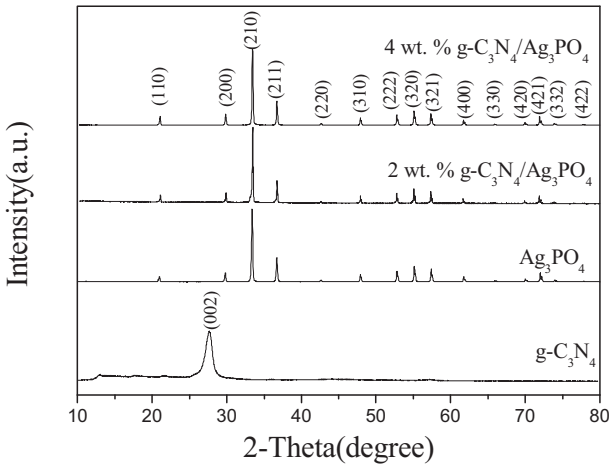

Fig. 1. X-ray diffraction patterns of the resulting products: pure Ag_3PO_4, pure g-C_3N_4, 2 wt.% g-C_3N_4/Ag_3PO_4 and 4 wt.% g-C_3N_4/Ag_3PO_4.